NUMERICAL SIMULATION OF GRANULAR CONVECTION:
EFFECTS ON PHOTOSPHERIC SPECTRAL LINE PROFILES

Åke Nordlund
Nordita, Blegdamsvej 17
Dk-2100, København Ø, Denmark

ABSTRACT

The results of numerical simulations of the solar granulation are used
to investigate the effects on photospheric spectral lines of the corre-
lated velocity and temperature fluctuations of the convective granular
motions. It is verified that the granular velocity field is the main
cause for the observed broadening and strengthening of photospheric spec-
tral lines relative to values expected from pure thermal and pressure
broadening. These effects are normally referred to as being due to "mac-
ro-turbulence" and "micro-turbulence", respectively. It is also shown
that the correlated temperature and velocity fluctuations produce a "con-
vective blue shift" in agreement with the observed blue shift of photo-
spheric spectral lines. Reasons are given for the characteristic shapes
of spectral line bisectors, and the dependence of these shapes on line
strength, excitation potential, and center to limb distance are discussed.

1. INTRODUCTION

Stellar as well as solar spectral lines are observed to be broader than
expected from purely thermal and pressure broadening. A weak Fe line at
$\lambda \simeq 500$ nm, observed at solar center disc, has a full width at half maxi-
mum (fwhm) of $\simeq 7$ pm or, expressed in velocity units $c\Delta\lambda/\lambda$, $\simeq 4.2$ kms^{-1},
whereas the value expected from pure thermal broadening is $2(\ln2)^{\frac{1}{2}}(2kT/m)^{\frac{1}{2}}$
$\simeq 2.0$ kms^{-1}. Close to the limb, at an angular inclination cosine, $\mu \equiv$
$\cos\theta = 0.16$, weak Fe lines have a width of $\simeq 6$ kms^{-1}. Classically, this
broadening is attributed to a "large-scale" velocity field, with assumed
Gaussian distribution, $\exp(-v^2/v_{macro}^2)$, of line of sight velocity. Typi-
cal required values of the "macro-turbulence" parameter are: $v_{macro} =$
$(v_{fwhm}^2/(4\ln2)-2kT/m)^{\frac{1}{2}} \simeq 2.2$ kms^{-1} at $\mu = 1$, $\simeq 3.4$ kms^{-1} at $\mu = 0.16$.

It is also well known that spectral lines are stronger than expected from purely thermal and pressure broadening of the line absorption profile. The concept of "micro-turbulence" was introduced to enforce a fit to the observed line strengths (Struve & Elvey 1934). Recently, accurate measurements of FeI oscillator strengths (Blackwell et al. 1975, 1976a, 1979a, 1979b) have made possible careful comparisons of observed and expected line strengths for a number of solar FeI lines, at several values of μ. If interpreted in terms of a "micro-turbulence" parameter, typical values required range from $v_{micro} = 0.6 - 0.9$ kms^{-1} at disc center, to $1.4 - 1.7$ kms^{-1} close to the limb (Blackwell et al. 1976b, 1979c).

Taken together, the broadening and strengthening data show that the velocity field responsible for the broadening cannot be a small scale velocity field; if so, it would give rise to more strengthening than is actually observed. As discussed previously (Nordlund 1976b, 1978), the convective granular velocity field is the likely candidate for this $2 á 3$ kms^{-1} velocity field, being on a bit too small scale to be fully spatially resolved observationally, yet on a large enough scale to show up mainly as broadening and only to a lesser extent as strengthening.

In a previous paper (Nordlund 1978) it was shown that the velocity field obtained from the equations of motion using an assumed, time-independent driving force, could be made to match both the broadening and strengthening of photospheric spectral lines if an appropriate horizontal scale and amplitude were chosen. The necessary size agrees well with typical granular sizes, and the necessary amplitude of the driving force is consistent with temperature fluctuations obtained in a simple, two-component model of granular convection (Nordlund 1976a).

Recently (Nordlund 1979) it has been possible to numerically solve the full set of hydrodynamical equations describing granular convection. In this treatment, the driving force is determined consistently from the energy equation, which governs the time-development of the temperature. Motions are allowed on a range of scales. The result is a realistic simulation of the granular convection. Results of these simulations are used in this paper to verify that the granular convection is the main cause of the broadening and strengthening of photospheric spectral lines (Section 3). The physical and numerical limitations of the simulations relevant to the spectral line formation problem are discussed in Section 2. Spectral line bisectors are discussed in Section 4 as a diagnostic tool to analyse the finer details of the granular convection. Section 5 summarizes the discussion.

2. THE NUMERICAL SIMULATION OF THE GRANULAR CONVECTION

A description of the numerical simulations is given elsewhere (Nordlund 1979). However, some details relevant to the synthetic spectral line calculations should be mentioned here:

The heavy computer storage and time requirements of three-dimensional hydrodynamic calculations naturally enforce strong numerical restrictions on the simulations. Allowing for 16×16 Fourier components in 16 layers, a compromise has to be made between spatial extent and resolution in the model. To cover the observed range of granular sizes (cf. Bray and Loughhead 1967, Fig. 2.1), the horizontal period was chosen = 3600 km. A vertical grid spacing of 100 km, with a vertical extent from $z = 1100$ km (depth relative to optical depth unity at $\lambda = 500$ nm) up to $z = -400$ km is a compromise between the vertical resolution rquired by typical scale heights $\simeq 150$ km in the photosphere; a large enough depth for the stratification to be almost adiabatic at the lower boundary, with small temperature fluctuations; and an upper boundary close to the top of the photosphere. This compromise was aimed primarily at a simulation of continuum brightness fluctuations for a computer movie. For the purpose of spectral line calculations, the upper boundary should preferredly have been placed at a somewhat higher level ($z \simeq -600$ km) to avoid influences from the necessarily imperfect boundary conditions.

Another important limitation concerns the energy balance in the line formation layers. The radiative part of the energy equation is necessarily handled with only a few wavelength points (typically three). However, the radiative part of the energy balance in optically thin regions is dominated by transfer in thousands of spectral lines. Energy is most efficiently exchanged between the gas and the radiation field at wavelengths where the optical depth is close to unity. This leads to a substantial cooling of the upper photosphere, relative to radiative equilibrium without spectral lines (spectral line "blanketing", cf. discussion in Gustafsson et al. 1975, Gustafsson 1979). Furthermore, radiative relaxation times in the line formation layers are typically underestimated by a factor of 5 - 10 when radiative transfer in the continuum alone is treated.

3. BROADENING AND STRENGTHENING OF PHOTOSPHERIC SPECTRAL LINES

For weak spectral lines, atoms see approximately the same radiation intensity regardless of local fluid + thermal velocity along the line of sight. Therefore, the strength of a weak spectral line averaged over horizontal area (and/or time) does not depend on the scale of the velocity field. The emergent average line profile simply reflects the distribution of line of sight velocities, convolved with the thermal velocity distribution. Thus, from the broadening data, one would estimate a ratio of horizontal to vertical velocities of approximately $3.4/2.2 \simeq 1.6$.

This velocity ratio is consistent with what would be expected of the velocity field of granules of typical dimensions. To see this, consider the condition of continuity applied to a simplified, one term representation of the granular velocity field,

$$\rho u_z = a(z)\cos(kx)\cos(ky) \qquad . \tag{1}$$

(In the numerical simulation a Fourier sum is used, but for the present illustration this single term suffices). The "anelastic" approximation to the continuity equation,

$$\text{div}(\rho\underline{u}) \simeq \text{div}(\rho\underline{u}) + \partial\rho/\partial t = 0 \qquad , \tag{2}$$

plus x-y symmetry, requires

$$\rho u_x = -a(z)/(2kH_a)\sin(kx)\cos(ky) \qquad , \tag{3}$$

$$\rho u_y = -a(z)/(2kH_a)\cos(kx)\sin(ky) \qquad , \tag{4}$$

where H_a is the scale height of the vertical mass flux amplitude $a(z)$, and $2^{\frac{1}{2}}\pi/k$ corresponds to the intergranular distance. Estimating $H_a \lesssim$ a density scale height $\simeq 140$ km, and $k \simeq 2^{\frac{1}{2}}\pi/1800$ km^{-1} (cf. Bray & Loughhead 1967, Tab. 2.1), one obtains $u_x^{rms}/u_z^{rms} \gtrsim 1.4$, in good agreement with the broadening of weak spectral lines.

The results of the numerical simulations of the solar granulations (Nordlund 1979) have been used to calculate synthetic spectral lines as averages over the simulation sequence (2 hours solar time) and area ($3600\times3600 \simeq 5\times5$ arc sec). Local thermodynamic equilibrium (LTE) was assumed, and pressure broadening was calculated according to Unsöld (1955) (with no

enhancement factor). The time averaging was performed as a sampling with
a 6 minute sampling interval. The horizontal averaging was performed using
bundles of 256 parallel rays, through all the grid points at z = 0.

An example of the granular velocity and temperature field is given in Fig.
1. In Fig. 2, observed full widths at half maxima of photospheric spectral
lines are compared with widths of synthetic spectral lines. The good agree-
ment in Fig. 2 shows that the granular velocity field (which is required
to transport the bulk of the solar energy output to the surface) does have
the average horizontal and vertical velocity amplitudes required to fit
the broadening data.Note, however, that the broadening at center disc is
slightly too small and that the broadening close to the limb is slightly
too large. These discrepancies are probably due to the neglect of the spec-
tral line blanketing in the numerical simulations. In the upper photo-
sphere, temperature fluctuations are induced by convective motions over-
shooting into a stable region. These temperature fluctuations tend to re-
tard the motion. If spectral line blanketing were correctly allowed for,
the temperature fluctuations would be reduced in magnitude (cf. the dis-
cussion in Section 2), and the retardation would decrease. Vertical velo-
cities would then decrease less rapidly with height, and the horizontal
velocities would be reduced, as required by the condition of continuity
(cf. discussion above, Eqs (1) - (4)). Attempts are presently being made
to include spectral line blanketing in a schematic way with a very small
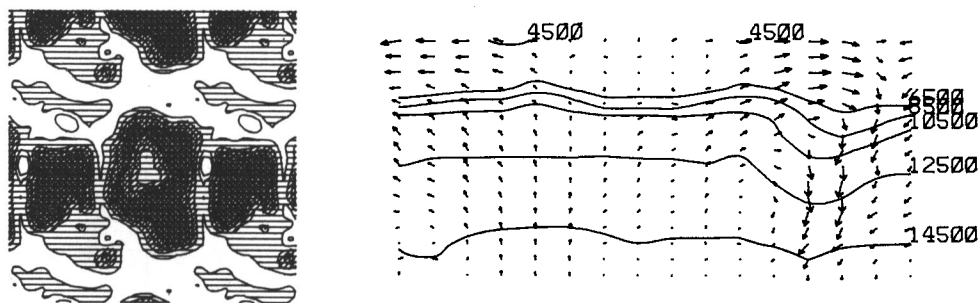number of wavelength points.

Fig. 1. The granular temperature field at z = 0 and the granular velocity
field in an yz-plane through the center of the center granule, at a time
when this granule has expanded to form an "exploding" granule. The tempe-
rature plot (left) is shaded above 6500 K, with the shading increasing in
steps of 1000 K. The velocity (right) is shown over the 3600×1500 km ver-
tical plane, with arrows showing the distance covered in 15 seconds. Tem-
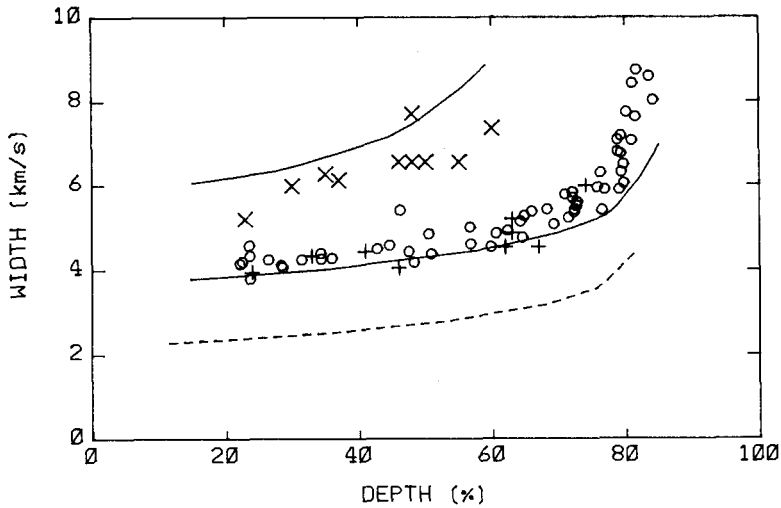perature contours are labelled with the temperature in K.

Fig. 2. Observed and calculated widths (fwhm) of solar FeI lines, as a function of line center depth, at $\mu = 1$ and $\mu = 0.16$. Observations are from Evans et al. (1975), for $\mu = 1$ (+) and for $\mu = 0.16$ (x); and from Stenflo & Lindegren (1977), for $\mu = 1$ (o). Synthetic spectral lines were calculated using $\lambda = 500$ nm and $\chi_{exc} = 3$ eV (which is typical for the observed lines). Full drawn lines show the results obtained (at $\mu = 1$ and 0.16) from an average (see text) of a 2 solar hour simulation of the solar granular convection. The dashed line shows widths expected at $\mu = 1$ (these are similar at $\mu = 0.16$ for small depths) with only thermal and pressure broadening.
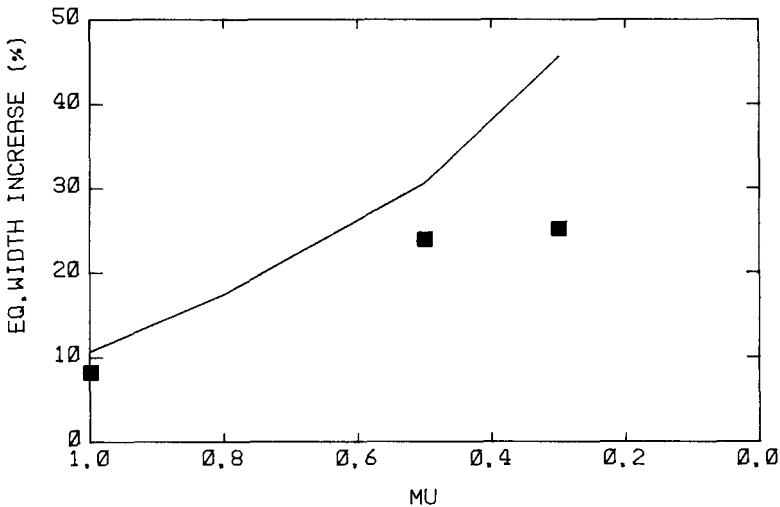

Fig. 3. The strengthening of a saturated FeI line, with $\lambda = 500$ nm, $\chi_{exc} = 1$ eV, and equivalent width 5 pm, as a function of μ. The full drawn line shows the equivalent width increase of the spectral line in the simulated granular velocity field, relative to equivalent width obtained with the velocity set to zero. The squares show the equivalent width increases corresponding to the "micro-turbulence" parameter values derived by Blackwell et al. (1979c) for similar lines.

In Fig. 3, the spectral line strengthening effects of the granular veloci-
ty field are illustrated. Traditionally, the observed and calculated equi-
valent widths of spectral lines are reconciled using a "micro-turbulence"
parameter. Thus, Blackwell et al. (1976b, 1979c) interpret their accurate
data on line strengthening in terms of an angle-dependent "micro-turbu-
lence", $v_{micro}(\mu)$. In Fig. 3, the line strengthening due to the simulated
granular velocity field is compared with that of the "micro-turbulence"
derived by Blackwell et al. It is obvious that the simulated granular ve-
locity field has a line strengthening effect similar to the one required
by the observations. The effects of the simulated granular velocity field
are too large towards the limb, just as was the case for the broadening
data.

The line strengthening effect of the granular velocity field is due to
gradients of the velocity along the line of sight. In the approximately
exponential photosphere, the optical length scale

$$\ell_\tau = ds/d\ln\tau = (dz/d\ln\tau)/\mu = H_\tau/\mu \tag{5}$$

is approximately inversely proportional to μ. Thus, in terms of optical
depth along the line of sight, velocity fluctuations appear to occur on
a smaller scale for inclined lines of sight. In itself, the granular velo-
city field is not isotropic; as discussed above, the horizontal velocities
are generally larger than the vertical ones (cf. also Fig. 1). Together,
these circumstances contribute to the the increased line strengthening
("micro-turbulence") towards the limb. In fact, as with the line broade-
ning, the line strengthening at small μ may be reproduced by a simple,
stationary, one-mode model of the granular velocity field (Nordlund 1976b,
1978). However, at disc center, line strengthening occurs mainly as a re-
sult of the velocity gradients associated with the time dependence of the
granular motions.

4. CONVECTIVE BLUE SHIFTS AND SPECTRAL LINE BISECTORS

Photospheric spectral line profiles show a net blue-shift because of the
larger contributions to the emergent intensity of the bright granules, with
their locally blue shifted spectral lines. Observationally, this blue shift
is known to be of the order 300 - 400 ms^{-1} for weak FeI lines, decreasing
with increasing line strength, and with a weak dependence on excitation
potential (e.g. Beckers & de Vegvar, 1978). Moreover, the blue-shifted

spectral line profiles are asymmetric (Adam et al., 1976). A concise and powerful way to present the blue-shift and asymmetry of spectral lines is to use the spectral line bisectors; i.e., the loci of points midway between equal intensity points on either side of the line profile (Adam et al. 1976, Dravins 1979, Dravins et al. 1979). The shape of the spectral line bisector reflects, in a complicated way, an average of the thermal and velocity fluctuations of the photosphere. With the wealth of spectral lines available, spanning a range of different elements, strength, excitation potential and wavelength, the ensemble of spectral line bisectors form - in a way - a "fingerprint" of the temperature and velocity fluctuations of the photosphere.

Fig. 4 shows bisectors of weak FeI lines, synthesized as above, using the results of the numerical simulations of the solar granulation. The order of magnitude of the shifts, the shapes of the bisectors, and the weak dependence on excitation potential are all consistent with the properties of observed photospheric spectral lines (Dravins 1979, Dravins et al. 1979). For stronger spectral lines, the agreement is less satisfactory. Again, this is probably a consequence of the numerical inadequacies of the upper photospheric region of the simulation model (cf. section 2).
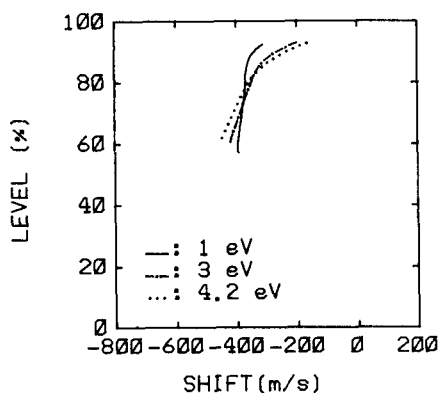

Fig. 4. Spectral line profile bisectors, for spectral lines with λ = 500 nm, line center depths $\simeq$ 40 %, χ_{exc} = 1 eV (full drawn), 3 eV (dashed), and 4.2 eV (dotted). Synthesized line profiles as in Figs 2 and 3.

To investigate some of the mechanisms influencing the shape of the bisectors, some calculations were performed with simpler velocity and temperature models. One of the important qualitative properties of the granular velocity field is its distinct asymmetry with respect to up and down: Granules with upward velocities are separated by narrow intergranular lanes with relatively larger downward velocities. This influences the shape of the bisectors in a characteristic way which is illustrated in Fig. 5. Due to the large red-shifts in the intergranular lanes, as compared to relatively smaller blue-shifts in the granules, the red wing of the average line profile is strengthened relative to the blue wing. An alternative way to see this is to consider the idealised case of a very narrow (δ-function) local line profile. The average spectral line profile then has the shape of the distribution function for the vertical velocities. The granular/intergranular asymmetry mentioned above corresponds to a distri-

bution function with an extended "red"
tail. This is the major cause of the
upper redward bend of the spectral line
bisectors. Fig. 5 illustrates how the
characteristic C-shape of the bisector
vanishes when the granular velocity field
is replaced by a velocity field of simi-
lar $v_{rms}(z)$, but with a purely sinusoidal
horizontal variation (and thus symmetri-
cal with respect to up and down). A depth-
-independent velocity amplitude, chosen
consistent with the line broadening data
results in approximately the same shift
as with the depth-dependent velocity amp-
litude, but with a different slope of the
bisector. A stronger penetration of the
temperature fluctuations up into the pho-
tosphere results in a smaller shift of
weak FeI lines. This is due to the strong
decrease in the number of FeI atoms with
increasing temperature, which results in
a weaker (in terms of equivalent width)
blue-shifted contribution.

Fig. 5. Bisectors of spectral
lines with λ = 500 nm, line
depths $\simeq$ 40 %, and χ_{exc} = 3
eV. The dashed line shows the
bisector obtained using a
quasi-stationary granular velo-
city field (cf. Nordlund 1978,
Fig. 6), and a parameterised
temperature fluctuation, ΔT =
$\Delta T_O(z-z_O)^2/z_O^2 \cos(kx)\cos(ky)$ for
$z > z_O$, ΔT = 0 for $z < z_O$, ΔT_O
= 1100 K, z_O = -100 km. The
dashed-dotted line shows the
bisector obtained with a velo-
city field with similar $v_{rms}(z)$,
but with a purely sinusoidal
horizontal variation, v =
$-2v_{rms}(z)\cos(kx)\cos(ky)$. The
full drawn line shows the bi-
sector obtained with a depth-
-independent velocity amplitude
= 2.5 kms^{-1} (v_{rms} = 1.25 kms^{-1}
). The dotted line shows the
bisector obtained with the gra-
nular velocity field, but with
ΔT_O = 1500 K, z_O = -300 km.

Fig. 6 illustrates the excitation poten-
tial dependence of bisectors of strong
spectral lines. The lower portions of
these bisectors show a reversed excita-
tion potential dependence; with higher
excitation potential resulting in a
smaller blue shift (in agreement with
the lower portions of observed bisectors of strong lines). These parts of
the bisectors are most influenced by the red flanks of the most blue-shif-
ted (granular) contributions to the average line profile. The radiation
intensities in these red flanks decrease strongly with excitation poten-
tial, both because of the Boltzman factor and because of the increased
pressure broadening.

Fig. 7 shows the center to limb behaviour of the bisector of a spectral
line selected to be similar to one of the three lines observed by Adam
et al. (cf. their Fig. 8). The C-shape of the bisector at center disc dis-
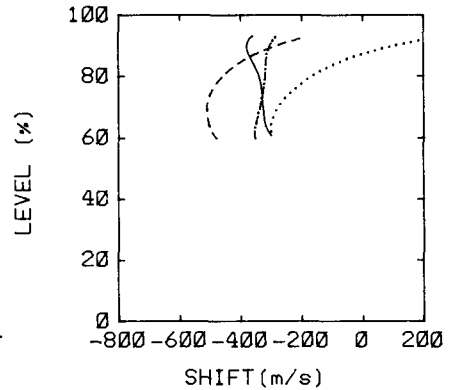appears as one approaches the solar limb. As discussed in connection with

Fig. 5, the C-shape at μ = 1 is caused by the up/down asymmetry of the line of sight velocity. For small μ, the line of sight is almost horizontal, and therefore the line of sight velocities are nearly symmetrical with respect to blue- and red-shift.

Fig. 6. Bisectors of strong spectral lines with λ = 500 nm and line center depths ≈ 80 %, for χ_{exc} = 1 eV (full drawn), 2.5 eV (dashed), and 4.2 eV (dotted). Synthesized with a granular velocity field and a parameterized temperature fluctuation, as in Fig. 5. ΔT_0 = 1100 K, z_0 = -100 km.

CONCLUSIONS

Numerical simulations of the solar granular convection show that the convective velocities in the solar photosphere are on the order of 1.5 kms^{-1} (typical rms vertical velocity) to 2.5 kms^{-1} (typical rms horizontal velocity). The broadening caused by this velocity field is consistent with the broadening of weak photospheric spectral lines. The velocities are also consistent with observed granular velocities corrected for limited spatial resolution (cf. the review by Wittman, 1979). Gradients of the granular velocity field are sufficient to explain the strengthening of photospheric spectral lines classically attributed to "micro-turbulence". The correlation of temperature and velocity in the granular convection causes a "convective blue-shift" and asymmetry of photospheric spectral lines. This is potentially, with sufficient accurate observations of stellar spectra, a powerful tool to investigate granular convection in stars other than the sun (cf. further discussion in Dravins et al., 1979).
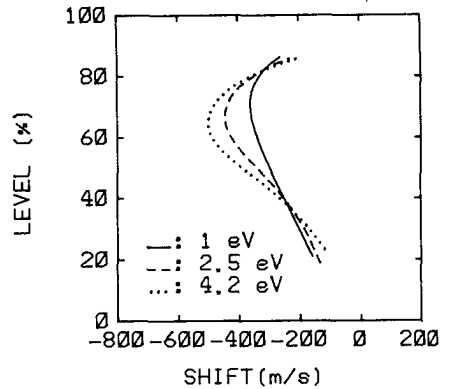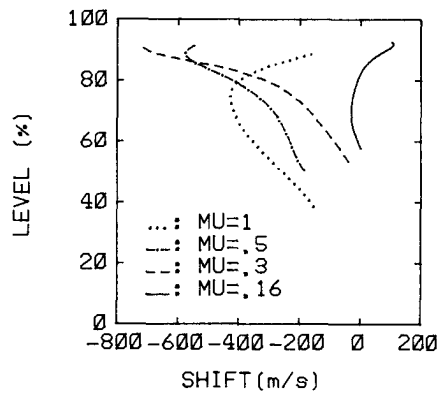

Fig. 7. Center to limb behaviour of the bisector of a spectral line with λ = 630 nm, line center depth ≈ 60 %, and χ_{exc} = 3.6 eV. Synthesized as in Figs 5 and 6. Compare Fig. 8 of Adam et al. (1976).

ACKNOWLEDGEMENTS

REFERENCES

Adam, M.G., Ibbetson, P.A., Petford, A.D.,1976, Monthly Notices Roy. Ast. Soc. 177, 687

Beckers, J.M., de Vegvar, P. 1978, Solar Phys. 58, 7.

Blackwell, D.E., Ibbetson, P.A., Petford, A.D., 1975, Monthly Notices Roy. Ast. Soc. 171, 195

Blackwell, D.E., Ibbetson, P.A., Petford, A.D., Willis, R.B., 1976a, Monthly Notices Roy. Ast. Soc. 177, 219

Blackwell, D.E., Ibbetson, P.A., Petford, A.D., Willis, R.B., 1976b, Monthly Notices Roy. Ast. Soc. 177, 227

Blackwell, D.E., Ibbetson, P.A., Petford, A.D., Shallis, M.J., 1979a, Monthly Notices Roy. Ast. Soc. 186, 633

Blackwell, D.E., Petford, A.D., Shallis, M.J., 1979b, Monthly Notices Roy. Ast. Soc. 186, 657

Blackwell, D.E., Shallis, M.J., 1979c, Monthly Notices Roy. Ast. Soc. 186, 673

Bray, R.J., Loughhead, R.E., 1967, The Solar Granulation, Chapman & Hall Ltd., London

Dravins, D., 1979, this colloquium

Dravins, D., Lindegren, L., Nordlund, Å., 1979, in preparation

Evans, J.C., Ramsey, L.W., Testerman, L., 1975, Astron. Astrophys. 42, 237

Gustafsson, B., Olander, N., 1979, Physica Scripta, in press

Gustafsson, B., Bell., R.A., Eriksson, K., Nordlund, Å., 1975, Astron. Astrophys. 42, 407

Nordlund, Å., 1976a, Astron. Astrophys. 50, 23

Nordlund, Å., 1976b, in "Problems of Stellar Convection", Lecture Notes in Physics no. 71, ed. Spiegel, E.A., Zahn, J.P.

Nordlund, Å., 1978, in "Astronomical Papers dedicated to Bengt Strömgren", ed. A. Reiz, T. Andersen; Cop. Univ. Obs.

Nordlund, Å., 1979, this colloquium

Stenflo, J.O., Lindegren, L., 1977, Astron. Astrophys. 59, 367

Struve, O., Elvey, C.T., 1934, Astrophys. J. 79, 409

Unsöld, A., 1955, Physik der Sterneatmosphären, Berlin, Springer

Wittman, A., 1979, in "Small Scale Motions on the Sun", Mitteilungen aus
  dem Kiepenheuer-Institut 179